Received: 28 November 2017 | Revised: 20 February 2018 | Accepted: 21 March 2018
DOI: 10.1002/bit.26601

ARTICLE

WILEY BIOTECHNOLOGY BIOENGINEERING

Hollow microcarriers for large-scale expansion of anchorage-dependent cells in a stirred bioreactor

Ashkan YekrangSafakar[1] | Aylin Acun[2] | Jin-Woo Choi[1] | Edward Song[3] | Pinar Zorlutuna[2,4] | Kidong Park[1]

[1] Division of Electrical and Computer Engineering, Louisiana State University, Baton Rouge, Louisiana

[2] Bioengineering Graduate Program, University of Notre Dame, Notre Dame, Indiana

[3] Department of Electrical and Computer Engineering, University of New Hampshire, Durham, New Hampshire

[4] Department of Aerospace and Mechanical Engineering, University of Notre Dame, Notre Dame, Indiana

Correspondence
Kidong Park, Division of Electrical and Computer Engineering, Louisiana State University, Baton Rouge 70803, LA.
Email: kidongp@lsu.edu

Funding information
National Science Foundation, Grant numbers: 1530884, 1611083, 1651385; Louisiana State University Board of Supervisors, Grant number: LIFT-15A-11

Abstract

With recent advances in biotechnology, mammalian cells are used in biopharmaceutical industries to produce valuable protein therapeutics and investigated as effective therapeutic agents to permanently degenerative diseases in cell based therapy. In these exciting and actively expanding fields, a reliable, efficient, and affordable platform to culture mammalian cells on a large scale is one of the most vital necessities. To produce and maintain a very large population of anchorage-dependent cells, a microcarrier-based stirred tank bioreactor is commonly used. In this approach, the cells are exposed to harmful hydrodynamic shear stress in the bioreactor and the mass transfer rates of nutrients and gases in the bioreactor are often kept below an optimal level to prevent cellular damages from the shear stress. In this paper, a hollow microcarrier (HMC) is presented as a novel solution to protect cells from shear stress in stirred bioreactors, while ensuring sufficient and uniform mass transfer rate of gases and nutrients. HMC is a hollow microsphere and cells are cultured on its inner surface to be protected, while openings on the HMC provide sufficient exchange of media inside the HMC. As a proof of concept, we demonstrated the expansion of fibroblasts, NIH/3T3 and the expansion and cardiac differentiation of human induced pluripotent stem cells, along with detailed numerical analysis. We believe that the developed HMC can be a practical solution to enable large-scale expansion of shear-sensitive anchorage-dependent cells in an industrial scale with stirred bioreactors.

KEYWORDS
anchorage-dependent cells, hiPSC, large-scale expansion, microcarriers, shear stress

1 | INTRODUCTION

With recent advances in biopharmaceutical industry and cell-based therapy, there is a strong need for efficient and reliable platforms to expand adherent cells in a large quantity. In biopharmaceutical industries, complex protein therapeutics and monoclonal antibodies are produced by various living organisms (Butler, 2005; Warnock & Al-Rubeai, 2006; Wurm, 2004). Especially, mammalian cells are often the preferred expression systems for producing complex biopharmaceutics (Sethuraman and Stadheim, 2006; Wurm, 2004), because they possess more human-compatible post-transcriptional metabolic machinery. Besides, a large amount of functional stem cells are required for various cell-based therapies which show a great potential to provide permanent cures for degenerative diseases (Daley & Scadden, 2008; Segers & Lee, 2008). Recent studies report efficacy of cell-based therapies on cardiac disease (Segers & Lee, 2008), cartilage repair (Brittberg, 2010), neurological disorder (Kim & De Vellis, 2009), bone damage and diseases (Cancedda, Bianchi, Derubeis, & Quarto, 2003), arthritis (Augello, Tasso,

Negrini, Cancedda, & Pennesi, 2007), and others (Daley & Scadden, 2008). Such stem cells are sensitive to the hydrodynamic shear stress (Dunlop, Namdev, & Rosenberg, 1994; Sethuraman & Stadheim, 2006; Wurm, 2004; Xing, Kenty, Li, & Lee, 2009) and is more challenging to expand on a large scale.

In laboratories, adherent cells are typically cultured with culture flasks with the surface area of 25–175 cm^2. However, large-scale cell expansion often requires over hundreds or thousands of such culture flaks, which is impractical due to the amount of the required labor. Roller bottles (Liu et al., 2003) or multilayer planar vessels (Bennett et al., 2012) can be used to provide much larger growth area of 1,000–10,000 cm^2. Using these for cell expansion tends to be an easy and direct translation from culture flasks, but they are still limited in their scale-up potential.

Currently, for large scale culture of adherent cells, a number of different platforms are available, such as microcarrier-based stirred bioreactors (Eibes et al., 2010; Hu et al., 2008; Lundgren & Blüml, 1998; Nam, Ermonval, & Sharfstein, 2007), packed-bed bioreactors (Looby & Griffiths, 1988), fluidized-bed bioreactors (Keller & Dunn, 1994), and hollow fiber bioreactors (Ku, Kuo, Delente, Wildi, & Feder, 1981). Among these, the microcarrier-based stirred tank bioreactors are widely used to culture a large population of cells that cannot survive as suspended single cells or cell aggregates. Anchorage dependent cells are grown on outer surfaces of suspended microcarriers, which are essentially solid microspheres. The microcarrier-based stirred tank bioreactors can expand and culture massive quantities of anchorage dependent cells in a single run.

As the capacity of a bioreactor increases, the surface-to-volume ratio of the cell suspension decreases. More vigorous stirring and aeration are required to maintain the mass transfer rate of nutrients and gases for larger number of cells (Xing et al., 2009). However, this increases hydrodynamic shear stress, which produces adverse effects on cells, such as reduced proliferation, low viability, and uncontrolled differentiation of stem cells (Croughan, Hamel, & Wang, 1987; Gupta et al., 2016; Leung, Chen, Choo, Reuveny, & Oh, 2010; Ng, Berry, & Butler, 1996; O'Connor & Papoutsakis, 1992). The trade-off between the mass transfer rate and the hydrodynamic shear stress makes large-scale expansion of shear-sensitive cells unreliable and leads to time-consuming optimization of operating conditions on each expansion stage, as those factors are typically affected by the bioreactor's capacity.

One of the approaches to address this issue is to optimize configuration and geometry of stirred bioreactors and their impellers for maximum media mixing and minimum hydrodynamic shear stress. Numerous studies (Cioffi et al., 2008; Dusting, Sheridan, & Hourigan, 2006; Grein et al., 2016; Odeleye, Marsh, Osborne, Lye, & Micheletti, 2014; Santiago, de Campos Giordano, & Suazo, 2011; Sucosky, Osorio, Brown, & Neitzel, 2004) made improvements to a certain degree, yet they cannot overcome the fundamental limits imposed by the finite diffusion rate of gases and nutrients and the hydrodynamics. Another approach is to locally shield cells from the hydrodynamic shear stress. This approach includes macroporous microcarrier (Ng et al., 1996; Nilsson, Buzsaky, & Mosbach, 1986), fiber discs in packed-bed reactors (Meuwly et al., 2006; Petti, Lages, & Sussman, 1994), and various encapsulation methods (Bauwens, Yin, Dang, Peerani, & Zandstra, 2005; Jing, Parikh, & Tzanakakis, 2010). Generally, in these techniques, cells are placed inside microstructures to be protected from the hydrodynamic shear stress (Martens et al., 1996). However, such protection make it difficult for nutrients and gases to reach the cells, as some of the cells are located deep inside the protective microstructures (Preissmann, Wiesmann, Buchholz, Werner, & Noe, 1997). Also, for the very same reason, it is very challenging to harvest the expanded cells.

In this paper, hollow microcarriers (HMCs) are presented, as a viable alternative to conventional microcarriers. HMCs are hollow microspheres and the target cells are attached to and cultured on the inner surface, as shown in Figure 1. Unlike conventional microcarriers, which directly expose cells to the external turbulent flow, HMCs protect the cells from the hydrodynamic shear stress. Meanwhile, openings on HMCs provide sufficient nutrients to the cells in them. As such, HMC will allow higher level of stirring and aeration in stirred tank bioreactors for increased culture capacity and density. As the protection mechanism is based on physical shielding, HMCs can be used universally for anchorage-dependent cells, including stem cells for tissue engineering and regenerative medicines as well as recombinant cells for biopharmaceutical industries. In this report, the fabrication process and numerical analysis of HMCs are presented, followed by the expansion of NIH/3T3 and the expansion and cardiac differentiation of human induced pluripotent stem cells (hiPSC).

2 | MATERIALS AND METHODS

2.1 | Fabrication of pre-stressed PDMS bilayer film

The fabrication process of HMC is presented in Figure 2a. A thick positive photoresist (AZ-9260, AZ Electronic Materials, Luxembourg, Germany) was spin-coated on a 4-inch silicon wafer at 1300 rpm for

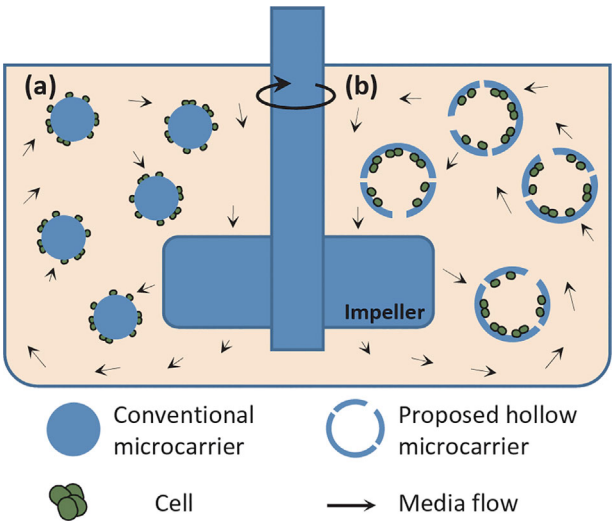

FIGURE 1 Working principle of hollow microcarriers (HMCs). (a) The cells on conventional microcarriers are exposed to the excessive shear stress. (b) As the cells are cultured inside the HMCs, they are protected from shear stress

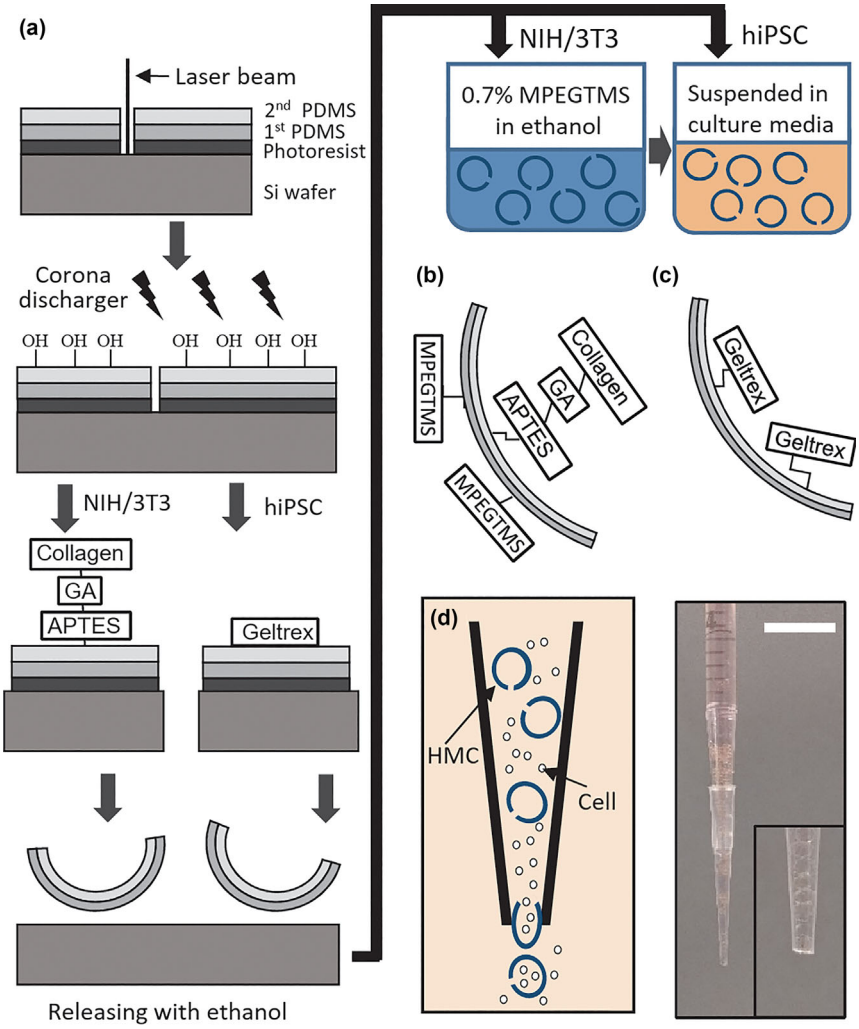

FIGURE 2 Fabrication process and seeding procedure of HMCs. (a) Schematic diagram of HMC fabrication process and surface treatment. Surface functionalization scheme of HMC for (b) NIH/3T3 and (c) hiPSC. (d) HMCs are seeded as they pass through narrow orifice with cells. Scale bar, 2 cm

10 s with target thickness of 13 µm and baked for 1 hr at 140 °C. Sylgard 184 (01064291, Dow Corning, Midland, MI) and Sylgard 3–6636 (01901443, Dow Corning) were mixed with mixing ratio of 5:1:3:3 ($Base_{184}$: Curing $agent_{184}$: Part-$A_{3\text{-}6636}$: Part-$B_{3\text{-}6636}$). The mixture was degassed in a vacuum chamber and spin-coated on the wafer at 2,000 rpm for 3 min with the target thickness of 18 µm. The wafer was baked at 40 °C overnight. The second layer of PDMS is a mixture of Sylgard 184 and Xiameter-200M (Dow Corning) with mixing ratio of 4:1:1 ($Base_{184}$: Curing $agent_{184}$: Xiameter). The mixture was degassed and spin-coated on the wafer at 1,300 rpm for 2 min with target thickness of 19 µm. The wafer was baked at 130 °C for 3 hr.

2.2 | Engraving and surface treatment

The patterns of HMCs were engraved on the pre-stressed PDMS film using a laser engraver (VLS 2.30, Universal laser system Inc., Scottsdale, AZ). The engraved film was treated with a corona discharger (BD-20, ElectroTechnic Products) to render it hydrophilic. Prior to NIH/3T3 fibroblast seeding, the wafer was immersed in an aqueous solution of 1% 3-Aminopropyltriethoxysilane (APTES) (440140, Sigma–Aldrich, St. Louis, MO) and incubated at 37 °C for 1 hr. After washing the wafer with PBS (phosphate buffered saline), the wafer was immersed in an aqueous solution of 0.1% glutaraldehyde (GA) (G5882, Sigma–Aldrich) for 20 min at room temperature, followed by rinsing with PBS twice. The film was then coated with collagen (A1048301, Life Technologies, Waltham, MA). The collagen was diluted with 0.2 M acetic acid to 50 µg/ml. The PDMS film was functionalized with the collagen solution at room temperature for 1 hr, followed by a PBS rinse. For hiPSC seeding, APTES and GA treatments were not necessary, as hiPSC cannot attach to unmodified PDMS. Geltrex (A1413201, Life Technologies) was diluted in DMEM (Dulbecco's modified Eagle medium, 11995040, Life Technologies) at 1% (v/v) and used to functionalize the PDMS film at room temperature. After 1 hr, the PDMS film was washed with PBS.

2.3 | Release process of HMC

The photoresist layer was dissolved by immersing the wafer in ethanol. After 6 min, the patterns on the PDMS film bent upward as being

released from the substrate. After complete releasing, they formed hollow microspheres or HMCs. The HMCs were collected in a 15 ml tube filled with ethanol. For NIH/3T3 fibroblast culture, HMCs were transferred to an ethanol solution of 0.7% (v/v) 2-[Methoxy-(Polyethyleneoxy)6-9Propyl]Trimethoxysilane (MPEGTMS) (65994-07-2, Gelest, Morrisville, PA) and kept in room temperature for 15 min. MPEGTMS was used to prevent cell attachment. It bounded only to the outside surface of HMCs, because most of the available OH groups on the inner surface were already reacted to APTES. Subsequently, HMCs were washed twice with ethanol. In order to transfer the HMCs to DMEM, the ethanol with HMCs was slowly added on top of a 15 ml tube filled with DMEM, to keep the layers of the ethanol and the DMEM separate. The HMCs were heavier than both ethanol and DMEM, causing them to slowly fall to the bottom of the tube. The ethanol was aspirated and the HMCs were washed with DMEM. For hiPSC culture, HMCs were rinsed with and stored in the m-TeSR-1 media (05850, StemCell Technologies, Vancouver, Canada), after releasing them with ethanol. Fully functionalized HMCs for the fibroblasts and the hiPSC are illustrated in Figures 2b and 2c.

2.4 | Numerical analysis

ANSYS Workbench (ANSYS Inc., Canonsburg, PA) was used to analyze the shear stress and the glucose concentration of a HMC with a confluent cell layer. To calculate the shear stress, CFX fluid flow module was used and the wall shear was calculated as a measure of the hydrodynamic shear stress on both sides of HMC. The HMC was fixed at the center of a cube with a 3 mm edge. The in-flow of 1 m/s was set at two opposite faces of the cubes and the out-flow condition was set at other two opposite faces. The mechanical properties of water were used for those of the culture media. The steady-state thermal analysis module was used to calculate the glucose concentration, as the mass diffusion equation is identical to that of the thermal diffusion equation. The cell concentration of 10^5 cells/cm^2, the glucose consumption rate of 1 ng/day/cell (Trummer et al., 2006), the glucose diffusivity of 9.58^{-10} m^2/s (Haynes, 2014), and the bulk glucose concentration of 4500 mg/L were assumed in the analysis.

2.5 | Cell culture

NIH/3T3 fibroblasts were maintained in cell culture flasks with DMEM supplemented with 10% (v/v) newborn calf serum (NBCS, 16010159, Life Technologies) and 1% (v/v) penicillin streptomycin (15140122, Life Technologies). The fibroblasts were subcultured every 5–6 days at 80% confluency. Prior to the experiment, cells were harvested using trypsin (25200056, Life Technologies) and counted.

The human fibroblast derived hiPSCs (DiPS-1016SevA, Harvard stem cell science, Cambridge, MA) were seeded on Geltrex (A1413202, ThermoFisher Scientific, Waltham, MA) coated tissue culture flasks using mTeSR-1 (05850, StemCell Technologies, Canada) supplemented with 5 μM ROCK inhibitor (Y-27632) (72302, StemCell Technologies) and maintained in mTeSR-1. At around 80% confluency, the hiPSCs were passaged using Accutase (07920, StemCell Technologies, Canada).

2.6 | HMC seeding and culture

The cell seeding procedure is shown in Figure 2d. For fibroblast seeding, the collagen coated HMCs were added to a cell suspension of 10^5 cells/ml. The cell suspension with HMCs was passed through a small orifice of 800 μm diameter, which was cut from a 200 μl pipette tip. As the HMCs passed through the orifice, they were temporarily squeezed and recovered to their original shape, allowing the cells to enter the HMCs. The seeded HMCs were placed over a cell strainer (10199–658, VWR, Radnor, PA) in a six-well plate to separate the cells that were not inside the HMCs. The HMCs were incubated for 6 hr in a static condition to promote cell attachment. Afterward, the HMCs were transferred to a spinner flask (CLS-1430-100, Chemglass, Vineland, NJ) with 100 ml of growth media and cultured under a humidified atmosphere of 5% CO_2 at 37 °C. The spinner flask was stirred by a slow-speed stirrer (440811, Corning Inc., Corning, NY).

For hiPSC seeding, the hiPSCs were collected using Accutase and a cell suspension of 10^6 cells/ml was prepared. HMCs were added to the cell suspension and seeded, following the same procedure as fibroblast seeding. The hiPSC seeded HMCs were then collected and maintained in mTeSR-1 in a static condition (24-well plates) or in a dynamic condition (30 rpm) provided by the same setup used for the fibroblasts.

2.7 | Proliferation assay protocol

The proliferation of the fibroblasts in the HMCs was characterized with Cell Counting Kit-8 (CK04, Dojindo, Kumamonto, Japan) following manufacturer's instructions. At the end of 3-hr incubation, the media was transferred into a separate 96-well plate to avoid optical interference of HMCs to the optical measurement. The proliferation of hiPSC in the HMCs were characterized in the static or dynamic culture conditions on days 1, 3, 5, 7, and 10 of culture, using alamarBlue assay (DAL110, Invitrogen, Waltham, MA) following manufacturer's instructions. We also used the phase-contrast images of HMC with hiPSC to manually measure the total areas of hiPSC colonies, to estimate the total cell number based on the cell concentration in colonies (see Supplementary information). The cell concentration in colonies was measured to be 7700 cell/mm^2. The HMCs with hiPSC were incubated for 6 hr at 37 °C, before transferring the media into a separate 96-well plate for the measurement. For both assays, the calibration curves were used to extract the cell number per HMC from the absorbance values at each time point.

2.8 | Cardiomyocyte differentiation of hiPSCs

hiPSCs on 2-D surfaces and in HMCs were differentiated into iCMs following a previously established protocol (Lian et al., 2013). Briefly, differentiation was started by incubating the hiPSCs in RPMI Medium 1640 (11875093, ThermoFisher Scientific) supplemented with B27 without insulin (A1895601, ThermoFisher Scientific), beta-mercaptoethanol (M6250, Sigma–Aldrich) and P/S (1%) (iCM basal media) with the addition of Wnt activator CHIR99021 (CHIR, 10 μM) (04–0004, Stemgent, Lexington, MA). On day 2, the media of the hiPSCs was

changed to iCM basal media without any CHIR. On day 4, Wnt inhibitor IWP-2 supplemented iCM basal media (5 μM) (04–0036, Stemgent) was introduced. On day 6, the media was changed to iCM basal media without any small molecules. On day 9 of differentiation, hiPCs were switched to iCM basal medium supplemented with B27 with insulin (17504044, ThermoFisher Scientific) and maintained in this medium from day 9 with media changes every 3 days. Beating was observed on day 12 of differentiation for iCM in HMCs and on 2-D surfaces.

2.9 | Quantitative reverse transcription polymerase chain reaction (q-RT PCR)

Total mRNA was collected from hiPSCs (day 4 after seeding) or iCMs (day 21 of differentiation) cultured in HMCs or on 2-D surfaces using an mRNA isolation kit (74104, Qiagen, Netherlands) following manufacturer's instructions. The collected mRNA was then reverse transcribed to cDNA using a cDNA synthesis kit (1708840, Bio Rad, Hercules, CA) following manufacturer's instructions. The cDNA was then used for the PCR reaction using a real time PCR (1725120, BioRad). The primers for NKX2.5 (assay ID: qHsaCED0001067, BioRad) and cardiac troponin-T (TNNT) (assay ID: qHsaCID0014544, BioRad) were purchased from BioRad. The sequences for NANOG and KLF4 primers were custom made (Eurofins, Luxembourg city, Luxembourg) and the corresponding sequences of KLF4 and NANOG are TATGACCCACACTGCCAGAA (forward)/TGGGAACTTGACCATGATTG (reverse) and CAGTCTGGACACTGGCTGAA (forward)/CTCGCTGATTAGGCTCCAAC (reverse), respectively.

2.10 | Immunostaining

hiPSCs (day 4 after seeding) or iCMs (day 21 of differentiation) cultured in HMCs or on 2-D surfaces were fixed using 4% paraformaldehyde (15710, EM Sciences, Hatfield, PA) for 15 min at room temperature. The cells were then permeabilized using triton X–100 (85111, ThermoFisher Scientific) (0.1%) for 20 min followed by a blocking step with goat serum (G9023, Sigma–Aldrich) (10%, 1 hr at RT). After blocking, the cells were incubated with primary antibodies against OCT-4 (MA1-104, ThermoFisher Scientific) or TNNT (ab45932, Abcam, Cambridge, MA) overnight (1:150 dilution in 10% goat serum, at 4 °C). After washing excess dye, the cells were incubated with the corresponding secondary antibodies (R37117, and A-11001, ThermoFisher Scientific) for 6 hr (1:200 dilution in 10% goat serum, at 4 °C). The nuclei of the cells were stained with DAPI. The samples were then mounted in anti-fade reagent (P36930, ProLong Gold, ThermoFisher Scientific) and imaged using a fluorescence microscope.

3 | RESULTS AND DISCUSSIONS

The geometry of HMCs determines the degree of protection from the hydrodynamic shear stress and the diffusion rate of nutrients and gases, as well as their mechanical integrity. Various geometries of HMCs were produced and tested, as shown in Figure 3 and Supplementary Figure S1. For efficient seeding, an HMC should be flexible enough to deform during the seeding procedure, in order to introduce cells into it. At the same time, it should be rigid enough to protect the cells from the hydrodynamic shear stress in bioreactors. We developed and tested a double hemisphere pattern, a linear pattern, and a snowflake pattern, as shown in Figure 3a–c. In this study, the snowflake pattern was used to produce HMCs. It had a center area with nine leaflets which bend and lean toward each other to form a sphere. The snowflake pattern produced a sufficiently rigid HMC which can maintain its tightness even when it is rotating in the spinner flask. At the same time, it can be squeezed to deform and introduce the cells into it during the seeding process. In order to fine-tune the performance of the HMCs, the snowflake pattern can be further modified. Additional openings can be made to enhance the exchange of media into the HMC by cutting the tip of the leaflets as shown in Figure 3d, or making side holes as shown in Figure 3e. Furthermore, the leaflets can be narrowed to adjust the opening gap between the leaflets, as shown in Figure 3f.

Also, HMCs can be created in different sizes as shown in Figures 3g and 3h. During the deposition of the PDMS layers, the film thickness was controlled by varying the rotation speed of the spin-coater, which resulted in HMCs with different diameters. The HMCs used in this study had a diameter of 1 mm, which was larger than typical microcarriers. The volume of the HMC was 0.52 μl, whereas the surface area was 3.14 mm^2, leading to the surface area to volume ratio of 60.4 cm^2/ml without considering the volume between HMCs in suspension. The surface area to volume ratio used with commercial microcarriers was in the range of 8–80 cm^2/ml (GE Healthcare, 2005) As shown in Figure 3g, the diameter of the HMC can be further reduced by changing the fabrication parameters. With sufficient miniaturization, the surface area to volume ratio of HMC can be increased to a similar level of commercial microcarriers.

For large-scale culture with HMC, the mass-fabrication of HMC is essential. Currently, HMCs are made of thin PDMS films, which are spin-coated on a silicon wafer. Although the fabrication process shown in Figure 2 was able to provide enough HMCs for the current study, it may not be sufficient for large-scale culture on an industrial scale. Batch processing with an automated spin-coater and wafer handlers will significantly increase the throughput and provide sufficient HMCs for billions of cells. Ultimately, for a successful commercialization, a roll-to-roll process that bonds and patterns two pre-stressed polymer films could be used to mass-produce HMCs.

A significant reduction in hydrodynamic shear stress on inner surfaces of an HMC and a negligible drop of glucose concentration in an HMC were confirmed with numerical analysis, as shown in Figure 4 and Supplementary Figure S2. The average shear stress on the outer surface was around 10 Pa and that on the inner surface was 1 Pa with the opening angle of 1°, which was the angle of the gap between leaflets. Although this number was based on the assumed media flow velocity as defined in the methods section, this simulation clearly showed that the shear stress was significantly reduced with HMCs. The glucose concentration in HMCs with a confluent cell layer was decreased by less than 2%, as shown in Figure 4b. We also

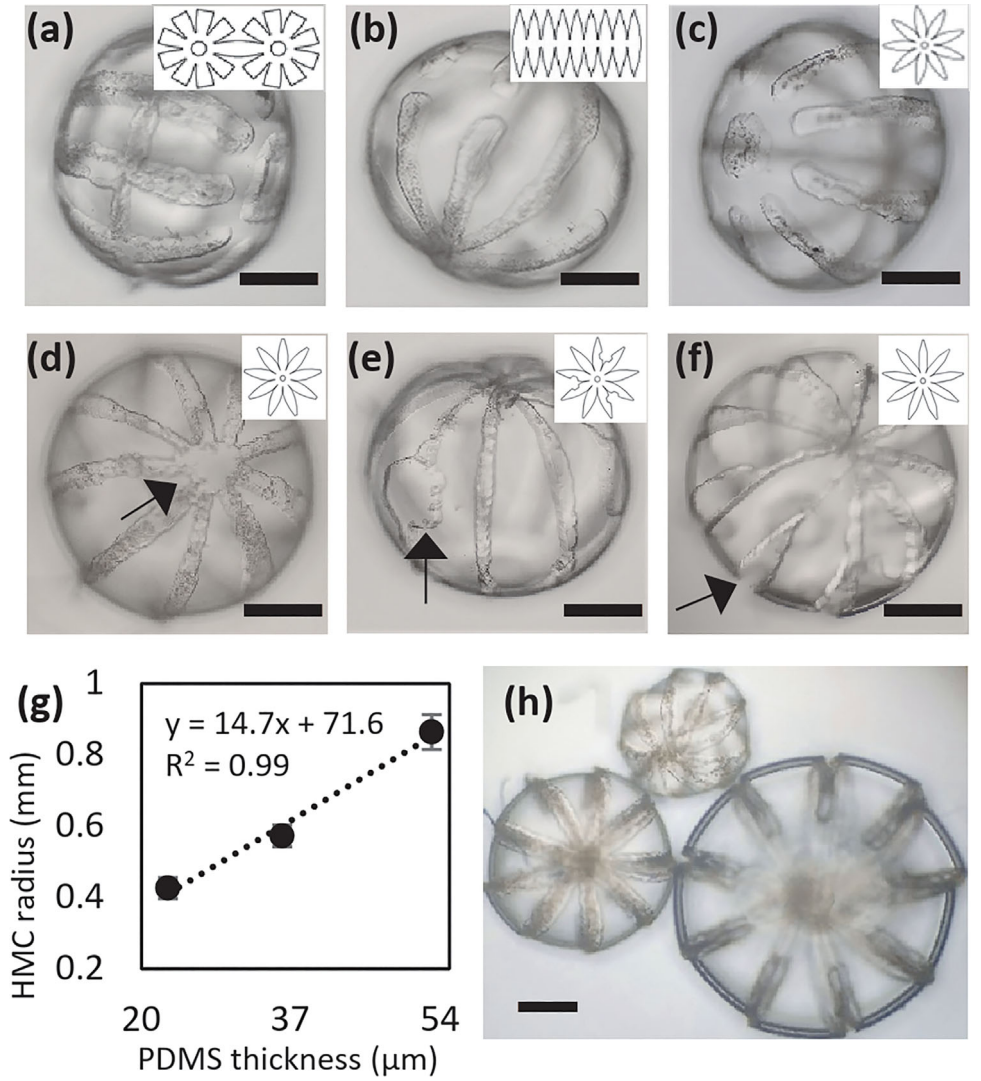

FIGURE 3 Geometry of HMC. HMCs made from (a) double hemisphere pattern, (b) linear pattern, and (c) snowflake pattern are presented. The snowflake pattern can be further modified to fine tune its performances, by (d) cutting the end of leaflets, (e) making side holes, and (f) increasing the gap between leaflets. (g) The size of HMCs can be controlled by changing the PDMS film thickness. (h) HMCs with the radius of 426, 573, and 864 μm. Scale bar, 300 μm

experimentally showed that the diffusion rate of the cell culture media into the HMC was high enough to support the active cell growth by a simple precipitation experiment (See, Supplementary Information). The shear stress can be further reduced by decreasing the gap between leaflets. However, this will reduce the diffusion of the glucose into the HMC and further decrease the glucose concentration. This tradeoff between the shear stress and the nutrient diffusion can be fine-tuned by varying the opening angle, as shown in Figure 4c. The HMC analyzed in Figures 4a and 4b has the opening angle of 1°. In an earlier work (Cherry & Papoutsakis, 1988), collisions with other microcarriers and the impeller of the bioreactor, and interaction with turbulent eddies were identified as major mechanisms for cellular damages. It was reported that the shear stress in the range of 10–200 Pa is lethal to cells and the shear stress in the range of 1–10 Pa can adversely affect the cell growth and protein production (Godoy-Silva et al., 2009). As the cells are inside the HMCs, they are protected from collisions with other HMCs and the impeller, as well as shear stress from the turbulent eddies.

Figure 5 shows the effect of MPEGTMS treatment on HMCs for NIH/3T3. Unlike hiPSC, NIH/3T3 can attach to unmodified PDMS in culture media. To prevent cell attachment on the outer surface, HMCs were immersed in ethanol solution of MPEGTMS, after the inner surface was functionalized with APTES, GA, and collagen, sequentially. MPEGTMS requires OH-groups to attach to PDMS. Since the available OH groups on the inner surface were already occupied by APTES, MPEGTMS only attached to outer surfaces, effectively preventing cell attachment on the outer surfaces. On the other hand, hiPSC cannot attach to a PDMS surface without Geltrex coating. Therefore, additional surface passivation was not necessary and Geltrex coating on the inner surface was sufficient. Figure 5a shows the difference between HMCs with and without MPEGTMS treatment. NIH/3T3 were cultured in HMCs for 6 days and the phase contrast images were

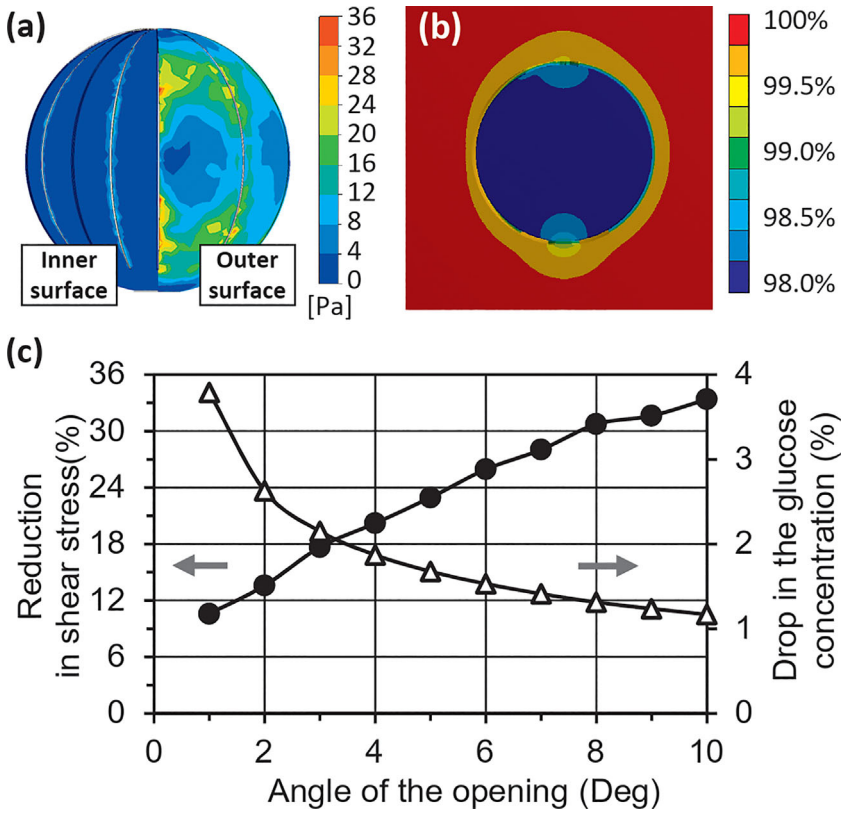

FIGURE 4 Numerical analysis on shear stress and glucose diffusion of HMC. (a) Shear stress is plotted. The left half of the HMC shows the shear stress on internal surface, whereas the right half shows that of external surface. (b) Concentration of glucose inside a HMC is decreased by 2%. (c) The reduction of the average shear stress and the drop in the glucose concentration can be fine-tuned with the opening angle of HMC. (The HMC in [a] and [b] has 1° opening angle)

taken. The focus was placed on the outer edge in the middle of HMC. The HMC with treatment had smooth edges, indicating no cells on the outer surface. The untreated HMC showed rough edges, due to the thickness of the cells on the outside surface. We also imaged HMCs using scanning electron microscopy (SEM). HMCs seeded with NIH/3T3 were fixed with formaldehyde and dried using hexamethyldisilazane. Prior to platinum sputtering for higher contrast in SEM, a few leaflets of HMCs were opened manually with tweezers to expose the inside. As shown in Figure 5b, the HMC with MPEGTMS treatment had no cells attached to the outside, whereas the cells on the inner surface show normal morphology of NIH/3T3 fibroblasts. On the other hand, HMCs without MPEGTMS treatment has the cells on both sides, as shown in Figure 5c.

The dynamic culture of NIH/3T3 was demonstrated with HMC, as shown in Figure 6. The fibroblasts inside the HMCs exhibited a multipolar and elongated shape, which is the typical morphology of actively proliferating fibroblasts, as shown in Figures 6a and 6b. Ideally, the number of the seeded cells in each HMC would be equal to the product of the HMC's volume and the concentration of the cell suspension used in the seeding procedure. However, we observed less number of cells in HMC after seeding. The number of the seeded cells calculated from the HMC's volume and the cell density was 52, whereas the actual seeded cell number was 40, leading to the seeding efficiency of 77%. We believe that a portion of the seeded cells left HMCs while they were being transported to the cell strainer after seeding. The proliferation rate of the fibroblasts in HMCs were characterized as shown in Figure 6c. The solid lines show the average cell number for each stirring condition while the dashed lines show individual experiments. Active proliferation of the cells was observed for 6 days with continuous stirring up to 90 rpm (revolution per minutes). In all of the conditions, the fibroblasts showed exponential growth over their culturing period except one data point on the last day at 42 rpm. The fold increase per day of fibroblasts for each stirring speed was calculated, as shown in Figure 6d. The fold increase per day was defined as $(C_f/C_i)^{1/D}$, where C_i, C_f, and D were initial cell count, final cell count, and days of expansion, respectively. The fold increase per day was stable up to 42 rpm and declined slightly at 70 and 90 rpm. It decreased significantly by very vigorous stirring at 150 rpm. The fold increase per day at 25 rpm was slightly larger than the static conditions. This can be attributed to the increased gas exchange in the media in the spinner flask as well as upregulation of the membrane proteins vital to cell proliferation (Senger & Karim, 2003). During the 6 days, the cells were expanded by 26.7 times at stationary condition, 29.7 times at 25 rpm, 28 times at 42 rpm, 7.1 times at 70 rpm, 7.3 times at 90 rpm, and 1.5 times at 150 rpm.

The recent advancements in stem cell research has introduced hiPSCs as a valuable cell source for acquiring various human-origin cell types without the ethical issues embryonic stem cells carry. hiPSCs are

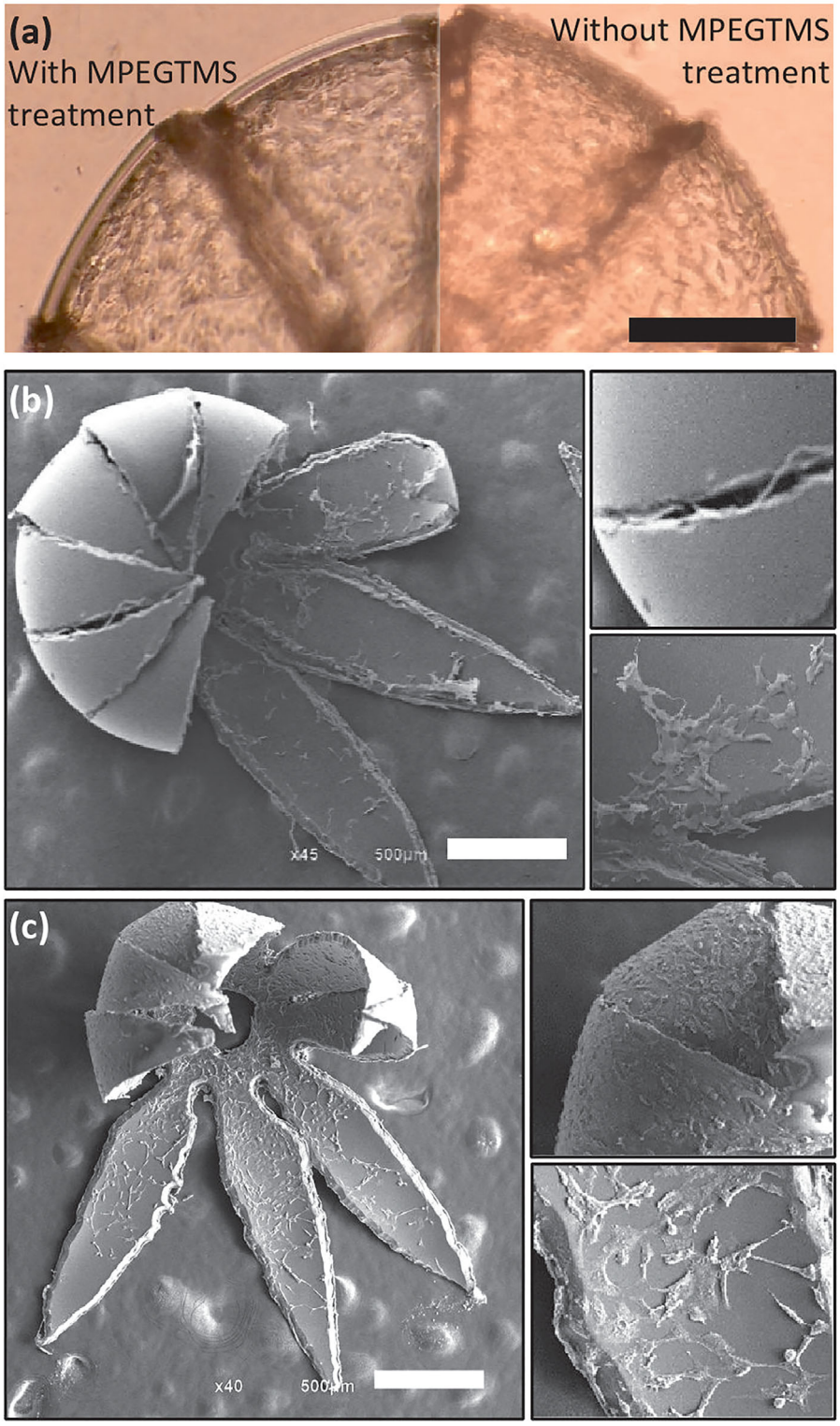

FIGURE 5 HMC surface treatment. (a) Phase-contrast images of HMCs treated with MPEGTMS (left half) and without treatment (right half) are presented. (Scale bar = 200 µm.) SEM image of HMC (b) with MPEGTMS and (d) without treatment. HMC with MPEGTMS treatment has cells only inside of HMC. Scale bar, 500 µm

especially valuable as a source for cell types that are not available from primary sources, such as cardiomyocytes. We cultured and expanded hiPSCs in HMCs and differentiated them to iCMs to explore the potential of HMCs for large-scale production of hiPSC-derived cells. We seeded the hiPSCs to Geltrex coated HMCs and achieved successful attachment, as shown in Figure 7a. The calculated initial cell number based on the HMC volume and the cell density of the cell suspension was 520 and the actual seeded cell number was 421 from

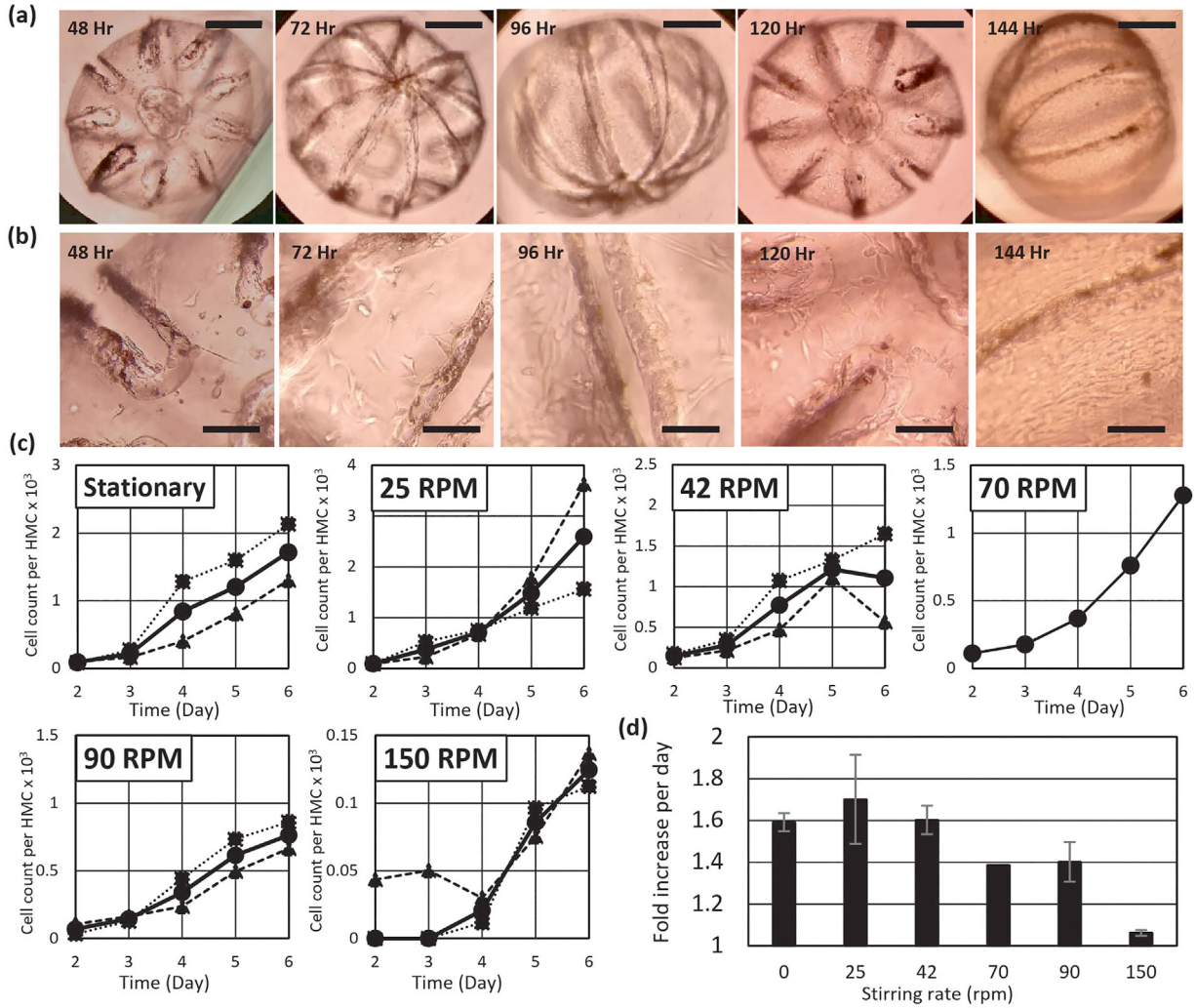

FIGURE 6 Proliferation and morphology of fibroblasts in HMCs. (a) Fibroblasts NIH/3T3 showed active growth in HMCs over 6 days. Scale bar, 300 µm. (b) Cell morphology is shown on each day. Scale bar, 100 µm. (c) Fibroblast NIH/3T3 were expanded in HMCs with different stirring rates and the cell number were counted daily. (d) Fold increase per day of fibroblast NIH/3T3 in HMCs with different stirring rate are presented

the image analysis of the seeded HMCs, leading to the seeding efficiency of 81%. The selective Geltrex coating on the inner surface of HMCs prevented cell attachment to the outside surface, evidenced by the smooth outer surface over a period of 10 days as shown in Figure 7a. Under both static and dynamic conditions, the hiPSCs were able to form the characteristic colony-like phenotype and proliferate inside the HMCs, as shown in Figure 7b. For dynamic culture of hiPSCs, stirring at 30 rpm was used. As the highest population increase of the fibroblasts was achieved on 25 and 42 rpm, we used a rotation speed within this range for hiPSC culture. As indicated by the cell number increase throughout the 10-day culture period, the hiPSCs can be successfully expanded in HMCs under dynamic conditions. In day 1 and 3, the number of the hiPSC measured with alamarBlue assay were higher than those from image analysis and also the maximum cell seeding density calculated form the volume (0.52 µl) of the HMC and the concentration of the cell suspension (10^6 cell/ml). We believe that low cell density of hiPSC in the HMC could bias alamarBlue assay. As with NIH/3T3, incubation under dynamic conditions induced a faster population growth when compared to static culture conditions. The calculated fold increase of hiPSC based on the alamarBlue assay at day 10 and the maximum cell seeding density was 24.17 and 17.72 times for dynamic and static condition.

We further characterized the healthy hiPSC phenotype by investigating their pluripotency. We determined if hiPSCs maintained their pluripotency in HMCs quantitatively and qualitatively, using q-RT-PCR and immunostaining, respectively. We observed that the hiPSCs cultured in HMCs showed similar mRNA expression of pluripotency markers KLF-4 and NANOG in comparison to ones cultured on conventional 2-D culture surfaces, as shown in Figure 7c. Similarly, the protein expression of another pluripotency marker, OCT-4, was comparable between hiPSCs cultured in HMCs and 2-D culture surfaces, as shown in Figure 7d. Overall, these results strongly suggest that HMCs are suitable platforms for fast and successful expansion of hiPSCs.

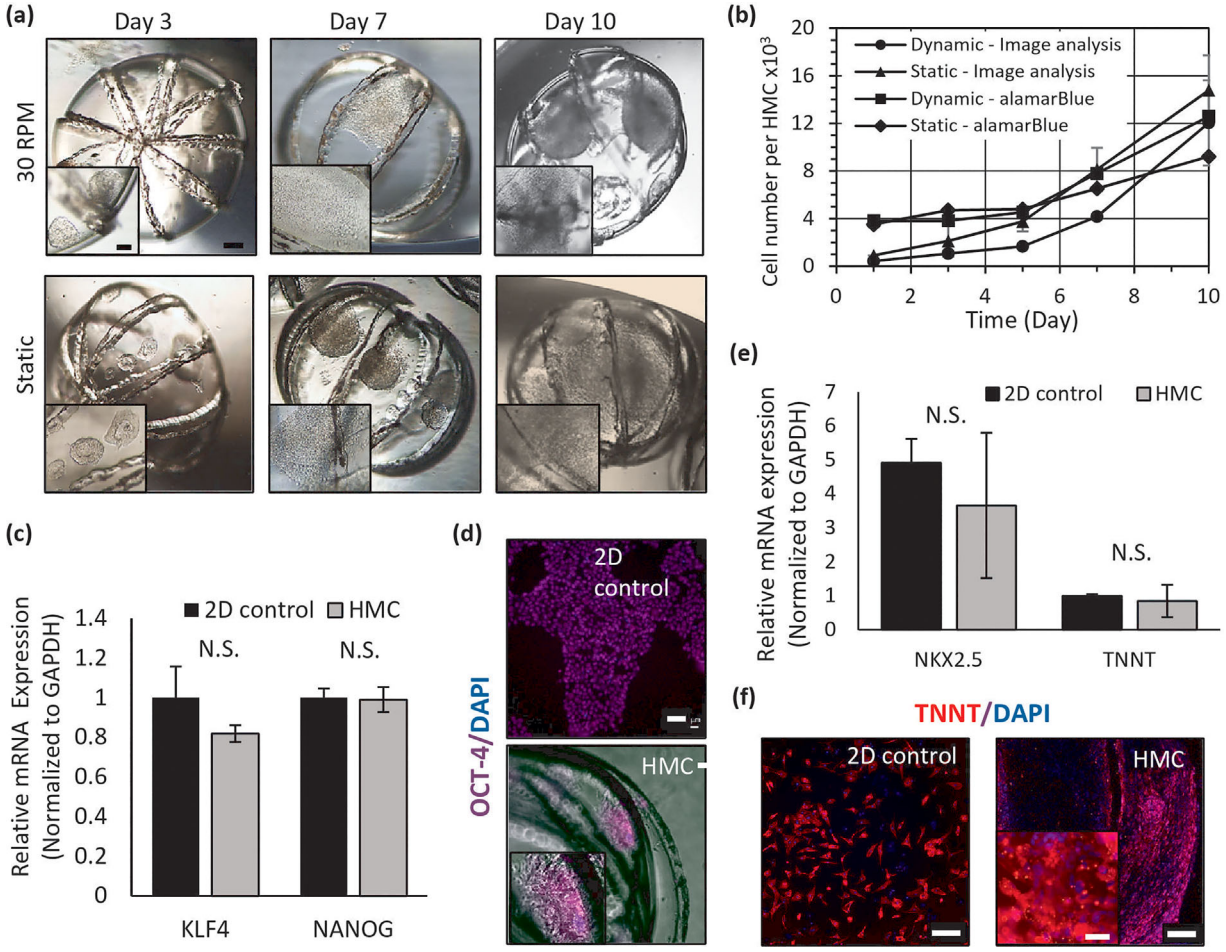

FIGURE 7 hiPSC growth expansion and differentiation with HMC. (a) Bright-field images of hiPSC seeded HMCs under dynamic (30 rpm) or static culture conditions. Scale bar, 200 µm. Inset scale bar, 50 µm. (b) hiPSC growth in HMCs under dynamic (30 rpm) and static culture conditions measured by alamarBlue assay and image analysis. (c) The q-RT PCR analysis showing mRNA expression of pluripotency markers KLF4 and NANOG in hiPSCs cultured in HMCs and 2D culture conditions. (d) The immunostaining of hiPSCs cultured in HMCs and on 2D glass surface against the pluripotency marker OCT4 (magenta). Scale bar, 50 µm. The differentiation of hiPSCs to cardiomyocytes in HMCs and on a 2D glass surface as shown by (e) the mRNA expression levels of cardiomyocyte markers NKX2.5 and troponin-T (TNNT), and (f) the immunostaining against cardiomyocyte marker TNNT. Scale bar, 100 µm. Inset scale bar, 20 µm. N.S. indicates no significance, $p > 0.05$

One of the crucial needs of stem cell research, tissue engineering, and regenerative medicine is large-scale and cost-effective production of mature and functional iCMs. After characterizing the hiPSC growth and functionality, we differentiated the expanded hiPSCs to cardiomyocytes while they were still growing inside the HMCs. At day 12 of the differentiation we observed beating iCMs (See Supplementary Figure S6 and Movie) in HMCs with the average beating frequency of 0.23 Hz, showing successful functional differentiation to cardiomyocytes. In addition, we characterized the iCMs for cardiac specific marker expression on both mRNA and protein level, as shown in Figures 7e and 7f. The q-RT-PCR showed that iCMs in HMCs express NKX2.5 and TNNT at comparable levels to iCMs cultured on conventional 2-D surfaces. Similarly, the positive immunostaining against TNNT in both HMCs and 2-D cultures further validated that differentiation in HMCs produced functional iCMs.

4 | CONCLUSION

In this paper, we presented the development of HMCs and the expansion and differentiation of NIH/3T3 fibroblasts and hiPSCs using HMCs, as a proof of concept. The developed HMCs effectively address the trade-off between the mass transfer rate of nutrients and the hydrodynamic shear stress in stirred bioreactors, that are widely used in biopharmaceutical industries. As the hydrodynamic shear stress is significantly reduced by HMCs, the production of shear-sensitive functional stem cells will be more robust and reliable. With further miniaturization of HMC for higher surface-to-volume ratio and development of high-throughput HMC fabrication setup, we believe that HMC can be a practical and efficient platform for large-scale expansion of adherent cells for biopharmaceutical industries and shear-sensitive stem cells for cell-based therapies.

ACKNOWLEDGMENTS

The authors would like to acknowledge support from the Louisiana State University Board of Supervisors (Award #: LIFT-15A-11) and the National Science Foundation (Award #1651385, #1530884, #1611083).

CONFLICTS OF INTEREST

The authors have no conflicts of interest to declare.

ORCID

Kidong Park http://orcid.org/0000-0003-1046-4645

REFERENCES

Augello, A., Tasso, R., Negrini, S. M., Cancedda, R., & Pennesi, G. (2007). Cell therapy using allogeneic bone marrow mesenchymal stem cells prevents tissue damage in collagen-induced arthritis. *Arthritis & Rheumatology*, *56*(4), 1175–1186.

Bauwens, C., Yin, T., Dang, S., Peerani, R., & Zandstra, P. W. (2005). Development of a perfusion fed bioreactor for embryonic stem cell-derived cardiomyocyte generation: Oxygen-mediated enhancement of cardiomyocyte output. *Biotechnology and Bioengineering*, *90*(4), 452–461.

Bennett, S. M., Cattadoris, H. J., Kenney, D. A., Martin, G. R., Tanner, A. J., & Wall, J. C. (2012). Multilayer cell culture vessels. US patent no: 8,178,345. May 15, 2012.

Brittberg, M. (2010). Cell carriers as the next generation of cell therapy for cartilage repair: A review of the matrix-induced autologous chondrocyte implantation procedure. *The American Journal of Sports Medicine*, *38*(6), 1259–1271.

Butler, M. (2005). Animal cell cultures: Recent achievements and perspectives in the production of biopharmaceuticals. *Applied Microbiology and Biotechnology*, *68*(3), 283–291.

Cancedda, R., Bianchi, G., Derubeis, A., & Quarto, R. (2003). Cell therapy for bone disease: A review of current status. *Stem Cells*, *21*(5), 610–619.

Cherry, R. S., & Papoutsakis, E. T. (1988). Physical mechanisms of cell damage in microcarrier cell culture bioreactors. *Biotechnology and Bioengineering*, *32*(8), 1001–1014.

Cioffi, M., Küffer, J., Ströbel, S., Dubini, G., Martin, I., & Wendt, D. (2008). Computational evaluation of oxygen and shear stress distributions in 3D perfusion culture systems: Macro-scale and micro-structured models. *Journal of Biomechanics*, *41*(14), 2918–2925.

Croughan, M. S., Hamel, J. F., & Wang, D. I. (1987). Hydrodynamic effects on animal cells grown in microcarrier cultures. *Biotechnology and Bioengineering*, *29*(1), 130–141.

Daley, G. Q., & Scadden, D. T. (2008). Prospects for stem cell-based therapy. *Cell*, *132*(4), 544–548.

Dunlop, E. H., Namdev, P. K., & Rosenberg, M. Z. (1994). Effect of fluid shear forces on plant cell suspensions. *Chemical Engineering Science*, *49*(14), 2263–2276.

Dusting, J., Sheridan, J., & Hourigan, K. (2006). A fluid dynamics approach to bioreactor design for cell and tissue culture. *Biotechnology and Bioengineering*, *94*(6), 1196–1208.

Eibes, G., dos Santos, F., Andrade, P. Z., Boura, J. S., Abecasis, M. M., da Silva, C. L., & Cabral, J. M. (2010). Maximizing the ex vivo expansion of human mesenchymal stem cells using a microcarrier-based stirred culture system. *Journal of Biotechnology*, *146*(4), 194–197.

Godoy-Silva, R., Chalmers, J. J., Casnocha, S. A., Bass, L. A., & Ma, N. (2009). Physiological responses of CHO cells to repetitive hydrodynamic stress. *Biotechnology and Bioengineering*, *103*(6), 1103–1117.

Grein, T. A., Leber, J., Blumenstock, M., Petry, F., Weidner, T., Salzig, D., & Czermak, P. (2016). Multiphase mixing characteristics in a microcarrier-based stirred tank bioreactor suitable for human mesenchymal stem cell expansion. *Process Biochemistry*, *59*, 266–275.

Gupta, P., Ismadi, M.-Z., Verma, P. J., Fouras, A., Jadhav, S., Bellare, J., & Hourigan, K. (2016). Optimization of agitation speed in spinner flask for microcarrier structural integrity and expansion of induced pluripotent stem cells. *Cytotechnology*, *68*(1), 45–59.

Haynes, W. M. (2014). *CRC handbook of chemistry and physics*. Boca Raton: CRC Press.

GE Healthcare. (2005). Microcarrier cell culture—Principles and methods. Available at: http://www.gelifesciences.co.kr/wp-content/uploads/2016/07/023.8_Microcarrier-Cell-Culture.pdf

Hu, A. Y. -C., Weng, T. -C., Tseng, Y. -F., Chen, Y. -S., Wu, C. -H., Hsiao, S., … Wu, S. -C. (2008). Microcarrier-based MDCK cell culture system for the production of influenza H5N1 vaccines. *Vaccine*, *26*(45), 5736–5740.

Jing, D., Parikh, A., & Tzanakakis, E. S. (2010). Cardiac cell generation from encapsulated embryonic stem cells in static and scalable culture systems. *Cell transplantation*, *19*(11), 1397–1412.

Keller, J., & Dunn, I. (1994). A Fluidized Bed Reactor for the Cultivation of Animal Cells. *Advances in Bioprocess Engineering: Springer*, 115–121.

Kim, S. U., & De Vellis, J. (2009). Stem cell-based cell therapy in neurological diseases: A review. *Journal of Neuroscience Research*, *87*(10), 2183–2200.

Ku, K., Kuo, M., Delente, J., Wildi, B. S., & Feder, J. (1981). Development of a hollow-fiber system for large-scale culture of mammalian cells. *Biotechnology and Bioengineering*, *23*(1), 79–95.

Leung, H. W., Chen, A., Choo, A. B., Reuveny, S., & Oh, S. K. (2010). Agitation can induce differentiation of human pluripotent stem cells in microcarrier cultures. *Tissue Engineering Part C: Methods*, *17*(2), 165–172.

Lian, X., Zhang, J., Azarin, S. M., Zhu, K., Hazeltine, L. B., Bao, X., & Palecek, S. P. (2013). Directed cardiomyocyte differentiation from human pluripotent stem cells by modulating Wnt/β-catenin signaling under fully defined conditions. *Nature Protocols*, *8*(1), 162.

Liu, Y., Wagner, K., Robinson, N., Sabatino, D., Margaritis, P., Xiao, W., & Herzog, R. (2003). Research report optimized production of high-titer recombinant adeno-associated virus in roller bottles. *Biotechniques*, *34*(1), 184–189.

Looby, D., & Griffiths, J. (1988). Fixed bed porous glass sphere (porosphere) bioreactors for animal cells. *Cytotechnology*, *1*(4), 339–346.

Lundgren, B., & Blüml, G. (1998). Microcarriers in cell culture production. *Bioseparation and bioprocessing: Biochromatography, membrane separations, modeling, validation*. Weinheim: Wiley-VCH.

Martens, D., Nollen, E., Hardeveld, M., van der Velden-De Groot, C., De Gooijer, C., Beuvery, E., & Tramper, J. (1996). Death rate in a small air-lift loop reactor of vero cells grown on solid microcarriers and in macroporous microcarriers. *Cytotechnology*, *21*(1), 45–59.

Meuwly, F., Loviat, F., Ruffieux, P. A., Bernard, A., Kadouri, A., & von Stockar, U. (2006). Oxygen supply for CHO cells immobilized on a packed-bed of Fibra-Cel® disks. *Biotechnology and Bioengineering*, *93*(4), 791–800.

Nam, J. H., Ermonval, M., & Sharfstein, S. T. (2007). Cell attachment to microcarriers affects growth, metabolic activity, and culture productivity in bioreactor culture. *Biotechnology Progress*, *23*(3), 652–660.

Ng, Y. C., Berry, J., & Butler, M. (1996). Optimization of physical parameters for cell attachment and growth on macroporous microcarriers. *Biotechnology and Bioengineering*, *50*(6), 627–635.

Nilsson, K., Buzsaky, F., & Mosbach, K. (1986). Growth of anchorage-dependent cells on macroporous microcarriers. *Nature Biotechnology*, *4*(11), 989–990.

O'Connor, K. C., & Papoutsakis, E. T. (1992). Agitation effects on microcarrier and suspension CHO cells. *Biotechnology techniques*, *6*(4), 323–328.

Odeleye, A., Marsh, D., Osborne, M., Lye, G., & Micheletti, M. (2014). On the fluid dynamics of a laboratory scale single-use stirred bioreactor. *Chemical Engineering Science*, *111*, 299–312.

Petti, S. A., Lages, A. C., & Sussman, M. V. (1994). Three-dimensional mammalian cell growth on nonwoven polyester fabric disks. *Biotechnology Progress*, *10*(5), 548–550.

Preissmann, A., Wiesmann, R., Buchholz, R., Werner, R., & Noe, W. (1997). Investigations on oxygen limitations of adherent cells growing on macroporous microcarriers. *Cytotechnology*, *24*(2), 121–134.

Santiago, P. A., de Campos Giordano, R., & Suazo, C. A. T. (2011). Performance of a vortex flow bioreactor for cultivation of CHO-K1 cells on microcarriers. *Process Biochemistry*, *46*(1), 35–45.

Segers, V. F., & Lee, R. T. (2008). Stem-cell therapy for cardiac disease. *Nature*, *451*(7181), 937.

Senger, R. S., & Karim, M. N. (2003). Effect of shear stress on intrinsic cho culture state and glycosylation of recombinant tissue-type plasminogen activator protein. *Biotechnology Progress*, *19*(4), 1199–1209.

Sethuraman, N., & Stadheim, T. A. (2006). Challenges in therapeutic glycoprotein production. *Current Opinion in Biotechnology*, *17*(4), 341–346.

Sucosky, P., Osorio, D. F., Brown, J. B., & Neitzel, G. P. (2004). Fluid mechanics of a spinner-flask bioreactor. *Biotechnology and Bioengineering*, *85*(1), 34–46.

Trummer, E., Fauland, K., Seidinger, S., Schriebl, K., Lattenmayer, C., Kunert, R., . . . Katinger, H. (2006). Process parameter shifting: Part I. Effect of DOT, pH, and temperature on the performance of Epo-Fc expressing CHO cells cultivated in controlled batch bioreactors. *Biotechnology and Bioengineering*, *94*(6), 1033–1044.

Warnock, J. N., & Al-Rubeai, M. (2006). Bioreactor systems for the production of biopharmaceuticals from animal cells. *Biotechnology and Applied Biochemistry*, *45*(1), 1–12.

Wurm, F. M. (2004). Production of recombinant protein therapeutics in cultivated mammalian cells. *Nature Biotechnology*, *22*(11), 1393.

Xing, Z., Kenty, B. M., Li, Z. J., & Lee, S. S. (2009). Scale-up analysis for a CHO cell culture process in large-scale bioreactors. *Biotechnology and Bioengineering*, *103*(4), 733–746.

SUPPORTING INFORMATION

Additional Supporting Information may be found online in the supporting information tab for this article.

How to cite this article: YekrangSafakar A, Acun A, Choi J-W, Song E, Zorlutuna P, Park K. Hollow microcarriers for large-scale expansion of anchorage-dependent cells in a stirred bioreactor. *Biotechnology and Bioengineering*. 2018;115:1717–1728. https://doi.org/10.1002/bit.26601